AN ACTIVE SOURCE EM METHOD FOR THE SEAFLOOR

C.S. Cox, T.K. Deaton and P. Pistek

Scripps Institution of Oceanography
La Jolla, California 92093 U.S.A.

ABSTRACT

An active source EM method has been used on the deep seafloor near the East Pacific Rise. The source consisted of an 800 meter long horizontal antenna grounded at the ends and supplied with 100 ampere excitation in a range of frequencies extending from 1/4 to 3 Hz. Power for the source was supplied from a surface ship. Receivers were autonomous units each detecting the horizontal components of the electric field by a crossed pair of 9 m antennas. The r.m.s. noise voltage in the receivers was several times greater than the thermal agitation noise in the electrode-to-sea water resistance of 4 ohms. Electromagnetic induction from turbulence induced by water flow past the electrodes may be a contribution to the excess noise. A signal/noise ratio of more than 20 dB was evident at a distance of 18.9 km from the source in a bandwidth of 2×10^{-3} Hz.

1. Introduction

The electrical conductivity of the ocean lithosphere remains almost entirely unknown because the lithosphere is relatively less conducting than the overlying ocean and the underlying asthenosphere. As a consequence of the oceanic shielding, only low frequency disturbances from above the surface can be expected to be present at the sea bed (Cox, 1980, 1981). The 5 km average depth of the deep sea is approximately one "skin depth" deep for EM oscillations of 5 minute period. Longer period oscillations are present at the sea bed but their interaction with the poorly conducting matter in the middle lithosphere is masked by the overwhelming reflection of EM disturbances from highly conducting layers below. The latter may be the asthenosphere underlying the lithosphere. Shorter period natural EM disturbances are present at the sea bed (fig. 1) but they are generated mainly by water currents of uncertain and probably small horizontal scale. They are consequently of little use for probing even moderately deeply into the lithosphere.

2. Choice of Methods

These remarks show the usefulness of introducing artificial EM fields from a known source on the sea bed (King *et. al.*, 1979, Cox, 1980, 1981). At first glance it may appear hopeless to detect artificial sources at useful distances from the transmitter because the highly conducting sea water will surely absorb most of the energy. The situation is however more favorable than one might guess for three reasons. (1) The signals can be encouraged to propagate along the more highly resistant, lithospheric half of the ocean-seafloor interface. (2) It is simple to couple energy rather efficiently both from the transmitter to the medium and from the medium to the receivers. This follows for electrically coupled systems from the favorable properties of highly conducting sea water in which electrodes are immersed. (3) The sea bed is remarkably free from geophysical noise sources at frequencies above one hertz. These advantages are illustrated in figure 2. In this figure, the horizontal electric and magnetic fields which reach the sea bed (after traveling

down-over-and up) are shown from a horizontal electric dipole (HED) source. Comparison is made with achievable noise levels. In constructing the figure, we have assumed that the permeability is everywhere uniform, that the conductivity distribution consists of homogeneous sea water overlying a homogeneous lithosphere, and that the receivers are colinear with the transmitter dipole and both are on the seafloor. In these circumstances the approximate analytical expressions for the horizontal field components on the seafloor at a distance r from the source are (fig. 2)

$$E_r = p \frac{F(\gamma_l r)}{2\pi \sigma_w r^3} \quad , \tag{1}$$

$$B_\phi = \frac{-\mu p F(\gamma_l r)}{2\pi \gamma_w r^3} \quad , \tag{2}$$

$$F(z) = (1 + z + z^2)\exp(-z) \quad , \tag{3}$$

$$\gamma = \sqrt{i \omega \mu \sigma} \tag{4}$$

where time dependence $\exp(i\omega t)$ is assumed and $p = I \delta L$ is the source dipole strength (current I times dipole length δL). In these expressions σ_l and σ_w are the conductivities of the lithosphere and water, respectively. The expressions are valid for

$|\gamma_w| >> |\gamma_l|$, $|\gamma_l^2 / \gamma_w| r << 1$, $|\gamma_w r| >> 1$ (see Wait, 1961 and Kraichman, 1970).

We note that, in the near field range where these expressions are valid, the attenuation with distance is controlled by F/r^3. At low frequencies $F \simeq 1$ and the expressions are equivalent to the $1/r^3$ behavior of a static dipole at the boundary of a half space of conductivity σ_w (Baños and Wesley, 1953). The factor F indicates that additional attenuation is entirely dependent on the conductivity of the lithosphere; i.e., the energy propagates *below* the ocean.

The indications (figs. 2 and 10) of receiver noise level for the electric field are actual measured values at the sea floor. The magnetic noise figures are from land measurements. They show

that only the superconducting magnetometer rivals a HED electric detector in sensitivity on the seafloor. The use of liquid helium cooling is naturally difficult on the seafloor (where does one vent the boiled off helium?). By comparison, electric detection is simple. These considerations indicate that an HED transmitter and HED receiver will be an effective combination. Another possibility must also be considered. It is conceivable to install a magnetic dipole transmitter. For comparison we consider the power which must be dissipated by the resistance of a loop antenna as compared with the power dissipated by an HED antenna. In fact, the fields along the axis of an electric dipole supplied with current I are equivalent to those of a *horizontal* magnetic dipole which is generated by the same current I flowing in a loop surrounding an area equal to the product of the length of the electric dipole by the skin depth (in sea water) at the frequency radiated. In this sense, the return flow of electricity through the sea avoids the expense (both in power and copper) of the complete loop of the magnetic dipole. A *vertical* magnetic dipole is less effective at generating distant fields (Chave and Cox, 1982). Furthermore, it is difficult to install a sufficiently large loop on the sea bed.

A complete HED system including transmitter and receivers was recently used during the Rivera Submersible Experiment (RISE) to study the electrical conductivity of the crust near the East Pacific Rise where it enters the Gulf of California (Spiess *et al.*, 1980; Young and Cox, 1981).

3. The Transmitter

The configuration of source and receivers adopted is shown in Figure 3. Electric power was supplied to the transmitter from a diesel generator on shipboard by transmission down an armored, coaxial cable. The same cable also provided a link for remote control of the transmitter.

Losses in the coaxial cable comprise ohmic loss caused not only by the transmission of the current necessary to drive the transmitter but also the current necessary to fill the capacitance of the coaxial cable. The latter is made small by choice of a low frequency source of electricity. In our case the power was transmitted at 60 Hz. The losses in the 10 km of cable (total capacitance 1 μFd, total resistance of central conductor 30 ohms) are primarily caused by the resistance in series with the load, not by capacitive current flow.

The transmitter power supply and driver were built into a pressure case and supported just above the seafloor. They consisted of a 7.5 kw transformer-rectifier set with SCR switches to provide unfiltered bipolar pulses of 100 A to the antenna. The wave form of voltage consisted of half cycle loops of the 60 Hz driving emf of one polarity modulated with a bipolar envelope as shown in fig. 4. The form of the envelope provides equal intensity on the fundamental and third harmonic of the repetition frequency. The condition for equality is

$$\sin \theta_2 = \sqrt{\frac{3}{2} - \frac{3}{4} \sin^2\theta_1} - \frac{1}{2} \sin\theta_1 \quad .$$

While maintaining this condition, one can vary the intensity of unwanted harmonics above the third by varying θ_1. The maximum efficiency for generation of the fundamental and 3rd harmonic occurs when $\theta_1 = 22.4775\ ^\circ$; $\theta_2 = 81.1077\ ^\circ$. If the envelope function modulated the half cycle loops of the ship's power precisely the voltage spectrum could be calculated simply by the convolution of the envelope spectrum by the spectrum of the half cycle loops. The latter consists of a line spectrum with lines at 0, 120, 240, 360, ... Hz with power proportional to 1/2 at n = 0 and $(4n^2 - 1)^{-2}$ for n> 0, where n = 1, 2, 3, ... is the order of the overtone. Because the envelope spectrum falls off rapidly wth increasing frequency, only the first term in the loop spectrum is of any importance so that the source spectrum is simply the product of the envelope spectrum by the loop spectrum at zero frequency. The fact that the envelope function did not modulate the half cycle loops precisely as described (because the SCR devices only turned off after their con-

duction current went to zero) leads to complications in the computation of the power in the fundamental and overtones as discussed by Young (1981).

The actual switching times of the envelope were controlled by an FM down-link (200 K Hz carrier) superimposed on the 60 Hz cable power. The repetition frequency was controllable in steps at 1/4 Hz, 1/2 Hz, 3/4 Hz and 1 Hz, and controlled accurately with a crystal controlled oscillator.

4. Transmitting Antenna

The antenna was constructed with insulated wire and electrodes made of bare sections at the ends of the antenna to enable return flow of the current. How long should the antenna be? The expressions shown in (1) are valid for infinitesimal δL.

One can consider the effect of increasing the length of the antenna by integrating the infinitesimal dipole contributions. From (1) it is apparent that the received electric intensity increases linearly with antenna length until the latter becomes comparable with the skin depth $\sqrt{2}\ /|\ \gamma_l|$ in the lithosphere. At greater lengths incremental increases no longer contribute signals of the same phase to the receiver. The skin depth in the *most* resistive medium is controlling because the energy is propagated horizontally only in this layer. A closely related fact is that the electric field is largely horizontal in the sea water but nearly vertical in the lithosphere. Therefore an electric antenna is far more efficient when laid horizontally at the bottom of the ocean than it would be if erected vertically in the water (Frieman and Kroll, 1973).

In the lithosphere we estimate the conductivity as 0.1 to .03 S/m in the basaltic upper crust and less within the lower crust. The skin depth is 2.9 km at 1 Hz in material of conductivity .03 S/m. Hence the antenna can be as long as 2.9 km without major interference effects which reduce its effectiveness. On the other hand, consideration of the cost of copper for the conductor show that this cost is practically independent of conductor length for constant dipole strength and power input. This follows as long as the radiation resistance of the antenna is negligible compared to its ohmic resistance. Let the latter be

$$R = \rho\ L\ /\text{cross sectional area} = \rho D\ L^2\ /M$$

where ρ, D are the resistivity and density of the copper, L is the length of the antenna and M the total mass of copper. The power required to drive current I is $W = I^2R$. Hence the dipole strength is $I\ L = \sqrt{\frac{WM}{\rho D}}$ independent of the antenna length.

These considerations neglect the cost of insulation (which favors a short, fat antenna conductor) and the resistance of the electrodes (which favors a long skinny one). We chose an 800 m antenna with a #2 gauge central copper conductor on the basis of these considerations and of an available winch and its capabilities. The antenna was insulated with a thermoplastic jacket and strengthened by a braid of high tensile steel wires since otherwise it might break under its own weight and drag while being raised from the sea bed. The inductive coupling between the antenna copper conductor and the braid lead to negligible losses in the antenna efficiency. Electrodes consisted of 10 m sections of 5/16 inch (0.8 cm) diameter aluminum rods securely connected to the far end of the antenna and to the center tap of the transformer power supply. The overall resistance of antenna and electrodes was 0.7 ohms. Hence a voltage and power of 70 V and 7 KW were sufficient to drive 100 A through the antenna.

Deployment of the antenna was carried out by lowering it while the ship moved slowly. The underwater transformer-rectifier set was connected to the end of the antenna closest to the ship and then the whole assembly lowered on the coaxial power cable which sent 60 Hz ship power to the set. An acoustic transponder was attached to the power coaxial cable 500 m above the transformer/rectifier unit. This was used together with three transponders in fixed positions on the sea bed for navigation. (The transponder navigation was carried out with great precision by the ANGUS team from the Woods Hole Oceanographic Institution.) It was possible to lay the antenna with a precision measured in a few tens of meters. An auxiliary acoustic pinger was attached just above the transmitter transformer. By controlling the winch it was possible to regulate the elevation of the pinger above the sea bed and thereby avoid raising the near end of the antenna off the seafloor or plunging the transformer pressure case into the bottom. During the duration of transmission, the ship was navigated to move slowly in the direction of desired antenna orientation, thus keeping the antenna stretched out.

Some motion of the antenna over the bottom being inevitable, it was necessary to choose a well sedimented bottom region on which to lay the antenna. Since the RISE crest is completely free of sediment, this requirement forced deployment to be away from the ridge crest, where sediments a few meters thick have accumulated in a narrow graben. The antenna was dragged several hundred meters over this sedimented bottom without damage.

5. Receivers

Three receivers were deployed. Since they were dropped free of any connection to the ship, they could be emplaced on rough, unsedimented, fresh basalt flows on the seafloor. The receivers (Figure 5) consist of two parts. One is a spherical pressure housing containing electronic components and sufficiently light to float the instrument back to the sea surface after completion of the experiment. The other part consists of ballast and plastic pipes which hold 4 electrodes forming a 9 m by 9 m horizontal cross antenna. This part was abandoned at the completion of measurements. The two parts were held together by a vacuum chamber. Explosive squibs, under control of timers, admitted water to the vacuum chamber thereby permitting separation. The electrical connection between antennas and the recorder package had to be severed when separation occurred. We made the connection through thin copper wires within the vacuum chamber. Hence they were in a water free environment during data collection, yet broke easily when the instrument housing floated free from its ballast anchor because they needed no insulation.

During deployment of a receiver, it was lowered from shipboard by a cable to which it was fastened by a command transponder. The accuracy of receiver positioning could therefore be as precise as the acoustic navigation of the transponder (about 10 to 20 meters). The transponder was commanded to release the receiver when the latter was about 1 km above the bottom but well below the influence of surface water currents which might deflect its fall. The receiver then sank at about 1 m/s to the bottom. Its orientation on the bottom (azimuth and tilt) was recorded by photographing a gimballed magnetic compass. The method of recording orientation

suffers from the disadvantage that the magnetic field may be severely disturbed around fresh basalt pillows on the seafloor.

Within the pressure case the receiver contained AC amplifiers for two components of the electric field, a data processing unit, a tape recorder, two timers (one redundant) for the vacuum release mechanism, the compass, and two beacon radio transmitters used during recovery.

Data processing consisted of digitizing the electric signals at 1/8 second intervals and "stacking" them so that the tape recorder saved primarily the mean signal obtained by summing successive four second cycles of data for 62 or 126 cycles. An additional 4 seconds of unstacked data were saved on tape after each transfer of stacked data to help understand any failures of the amplifiers or antenna system. Stacking of the data is equivalent to narrowing the bandwidth of harmonics of the 1/4 Hz stacking frequency. This emphasizes signals coherent with the stacking (therefore the transmitter frequencies) and discriminates against random noise. It also enables compression of the data so that several days' data can be stored on a small tape recorder. Some examples of unstacked and stacked records are shown in Figure 6.

6. Electrodes

Two types of electrodes were used in this experiment. The electrodes for the source transmitter had to handle large currents with a low voltage drop while the receiver electrodes had to connect the receiver antenna to the water with low noise. These different requirements are satisfied by electrodes of very different character although low resistance is needed for both. The effective resistance of a metal electrode (used in the transmitter system) or of an electrochemical cell (used for the receiver) is comprised of three parts, ohmic resistance within the seawater adjacent to the electrode, polarization at the interface between electrode and seawater, and ohmic resistance of the metal conductor within the electrode.

The first item can be called the geometric resistance because it depends on the geometry of the surface of the electrode.

We have considered three geometries of the substrate of the electrode: a sphere and a circular disk of radius a, and a prolate spheroid with semi-minor and semi-major axes a and c. If we consider each of these shapes immersed in a uniform fluid of resistivity ρ, we can compute their resistances R. The results are shown in Table I.

The cost of an electrode both in terms of money and in terms of generation of turbulent eddies and water drag depends approximately on its surface area A or volume V. As a rough indication of the merit of an electrode geometry, we have constructed two figures of merit, also listed in the table:

$$F_A = \rho / (RA^{1/2}) \qquad F_V = \rho / (RV^{1/3}) .$$

Inspection of the table shows that the disk electrode is superior to the sphere (because it has a higher figure of merit F_A) and a long prolate spheroid is superior to both. We have chosen an approximation of the last (a long cylinder) for both the transmitter and receiver electrode geometries. For the transmitter the important criteria were low resistance and small water drag. For the receiver, low resistance and small cost were important.

The actual electrode shapes are cylinders, not prolate spheroids. The difference is unimportant, and we have calculated approximate figures of merit for the transmitter and receiver electrodes (bottom rows of table). The values of a/c are equated to the diameter/length ratio of the metallic surface of the electrodes.

The other items influencing resistance are resistance of the metal conductor and the polarization resistance of the electrode. For the receiver electrodes the metallic conductor, silver, had negligible resistance and the polarization resistance will be described in a later paragraph. For the transmitter source electrodes both are important. The polarization loss is non-ohmic (time

dependent and nonlinear with respect to current). We found that 10 m sections of 8 mm diameter aluminum rod or 9.55 mm steel wire rope made good electrodes. At a frequency of 1/4 Hz the polarization voltage drop for each electrode was measured to be 2.2 v or less at a current density of 10 A/m of electrode length. The effective (linearized) conductance of the electrode per unit length is s = 4.5 S/m or less. Let the resistance of the metal (rod or wire rope) per unit length be r. Then the linearized equations governing electric current magnitude i and voltage v within the metal are

$$\frac{\partial i}{\partial x} = sv \text{ and } \frac{\partial v}{\partial x} = r\, i$$

where x is the distance measured along the electrode from its far end. The boundary conditions are $v = \mathrm{E}$ at the source where $x = L$ and $\partial v/\partial x = 0$ at $x = 0$. The solution is

$$i(x) = \mathrm{E}\sqrt{s/r}\,\{\cosh[L\sqrt{(rs)}]\}^{-1}\sinh[x\sqrt{(rs)}]$$

and the resistance at the source end is

$$R = \mathrm{E}/i(L) = \sqrt{(r/s)}\coth[L\sqrt{(rs)}]$$

These estimates show that optimizing the source electrode involves all three elements which contribute to the resistance, geometry, ohmic loss in the conductor and polarization loss. Estimates valid for the aluminum rod electrodes used in the Rise experiment are that the geometric resistance was .038 Ω and the combined polarization and ohmic resistance ($r = 5.9\times10^{-4}\,\Omega$/m, $s = 4.5$S/m, $L = 10$m) was $R = .068\Omega$ for a total of 0.11Ω for each electrode.

The ability to detect weak electric fields on the seafloor depends on achieving a very low noise level. Geophysical noises from ionospheric, ocean wave, seismic and acoustic sources are so low that they are not detectable by receivers using the short antenna length of 9 meters (Webb and Cox, 1982, 1984). Other sources are due to water motions, electrochemical effects in the

electrodes, thermal agitation and excess noise in the amplifiers. Turbulent water motions induce noise by interaction with the geomagnetic field. The turbulence can be generated by water flow past the electrodes themselves. In addition, there may be streaming potentials within the electrode itself. These effects are reduced by having the electrodes held down on the seafloor where water flow is minimal. We applied weights to the end of the antenna arms for this purpose. This also reduces the possibility of vibration of the arms by vortex shedding – a cause of noise induced in the antenna wires.

Thermal agitation noise is reduced by use of low resistance electrodes and lead-in wires. The electrodes consist of an electrochemical cell (Ag-AgCl) built on a rigid substrate. Their resistance is developed by polarization in the cell and by the geometric resistance. Noise and polarization resistance depend on the nature of the electrochemical cells.

A qualitative comparison of the level of noise for different types of electrodes (Pb - Pb SO_4, copper and its salts, Ag-AgCl) showed the Ag-AgCl system to be the best of those studied.

The properties and preparation of Ag-AgCl electrodes are well described in chemical literature (Ives and Janz, 1961) but our purpose was to measure very small electric potentials (of order 10^{-9} V) in the frequency band 0.1 - 10 Hz and these requirements are very different from the requirements of the chemist. Our aim was to build electrodes with low resistivity to increase the signal power relative to thermal noise, to reduce noise caused by water motion near the electrodes, and to keep construction to a reasonable cost.

A piece of silver mesh (#20) of rectangular shape (5 cm x 14 cm) with a piece of silver wire welded on it was cleaned in 30% $HN0_3$, bent around a plastic rod and then the rod was glued into a ceramic crucible (or cellulose extraction thimble) (Figure 7). The space between the mesh and thimble was tightly packed with a mixture of AgCl powder and diatomaceous earth in the ratio 1:5. The purpose of the AgCl is to ensure a saturated solution of Ag^+ ions close to the mesh. AgCl is surprisingly soluble in seawater. It is advantageous to add the diatomaceous earth

because agglomerated pieces of AgCl can be powdered with it in a mortar. This crucible was placed inside a larger one and the space between them was packed with diatomaceous earth. The earthy particles are small and homogeneous and do not contribute greatly to the resistivity of the system; at the same time they reduce the velocity of water flow through the electrode, and this seems to be advantageous in reducing one source of noise. The large crucible was made from sintered glass fibers. (Equally quiet electrodes have been made recently with porous polyethylene containers in place of the thimble and the glass fiber crucible.) The top cover was glued to the crucibles and to the rod, and finally the silver wire was soldered to the insulated copper wire which conducts the signal to the amplifier. The joint was covered with epoxy resin to isolate it from water. The whole system was protected from mechanical damage by a PVC cylindrical cover with large holes on all sides. The electrodes were placed in a vacuum which was vented by a NaCl solution (35g/l). This procedure removes air bubbles and maintains good contact between the silver mesh and the NaCl solution. The silver mesh was then electrolytically covered with AgCl as follows: the mesh was made an anode and a piece of silver was used as a cathode in NaCl solution (35g/l) and electrolyzed. The density of the electrolyzing current was 2mA per cm^2. The time of the electrolysis was 12 minutes. One result of electrolysis is production of hydroxide ions in the solution. To remove these ions a solution of HCl was used to neutralize them or the old NaCl solution was exchanged with new. After electrolysis, the resistivity of a pair of electrodes was measured for different frequencies (Figure 8) and after several hours of equilibration, potential differences between the pairs of electrodes were established (a pair of electrodes was considered acceptable if the potential between them was less than 1 m V).

From our earlier experiences with measurements of the electric field on the deep ocean bottom (Cox *et al.*, 1978; Pistek, 1977), we found that noise was reduced considerably by placing pieces of cloth around the electrodes. Water circulation over unprotected electrodes possibly caused disequilibria in electrochemical processes on the electrodes, generating an electric poten-

tial. Such effects may also be related to streaming potentials. At all events water motion on the electrodes increased the noise greatly. In our construction we have put two protecting layers (crucibles and diatomaceous earth) to reduce water circulation; thus packing with cloth is unnecessary.

Electrodes were tested for noise level in the laboratory. They were mounted close together near the bottom of an experimental nonconducting water tank filled with salt water. The voltage difference between them was amplified by the low noise amplifier described in Sec. 7. A noise level of 2 nV rms in the frequency band of 0.02 to 20 Hz was found. It was of the same order as the noise level of the amplifier. We conclude then that electrode noise was undetectable. A water current of 10 cm/sec over the electrodes or water motion caused by a propeller mounted over the electrodes and moving with different frequencies did not cause larger electric disturbance. Subsequent observations with a lower noise amplifier of the voltage between two closely spaced electrodes on the seafloor show that the noise approaches the thermal agitation limit above 2 Hz and at low frequencies rises faster than 1/f (Webb and Cox, 1984).

These electrodes have been used to detect with great sensitivity electrolytic processes at the surface of pieces of submerged bare iron or aluminum (at a distance of 0.5 m within the insulated tank). These processes generate a broad spectrum of electric noise. Therefore bare metal must not be mounted close to the antenna electrodes of the receiver.

The construction technique described is suitable for low noise electrodes in the frequency band 0.1 - 100 Hz; it is cheap because the amount of AgCl needed is reduced by mixing it with the diatomaceous earth.

7. Low Noise Amplifier

Two horizontal components of the electric field were amplified with a voltage gain of 4 x 10^6 over a frequency band extending from 0.15 Hz to 3 Hz (the gain drops rapidly beyond 2 Hz to avoid aliasing). Our sampling frequency was 8 per second. In order to achieve low noise at an input impedance of 4 ohms, we have used an impedance matching transformer at the input. The specially designed transformer has a 1:50 step up turns ratio and is able to operate at frequencies above 0.1 Hz (Figure 9).

The transformer is saturated easily so it was necessary to block the millivolt level offset between electrode pairs with a large (20,000 to 180,000 μFd) computer grade electrolytic capacitor. Capacitor polarity need not be observed at these low voltages.

The signal from the transformer secondary was chopped by a CMOS switch with a typical "on" resistance of 180 Ω. We were pleased to discover that the noise contributed by the switch does not significantly exceed that which would be expected from the thermal noise of its "on" resistance. The signal was chopped in order to shift its frequency spectrum to a point where the IC op amp noise is at a minimum. Chopping also permitted most of the amplification to take place in an AC amplifier stage, eliminating drifts caused by thermo-couple effects or by the amplifier itself.

The first stage amplifier was a very low noise op amp operating with a voltage gain of almost 3000. It was followed by a micropower op amp operating as a synchronous detector, its gain being switched between plus and minus one by the FET driven by the chopping voltage.

The detected signal was further amplified by another low power op amp whose associated RC networks attenuate frequencies below 0.15 Hz and above 5.5 Hz. The overall voltage gain from the electrodes to this point was 125 dB.

Finally the fluctuating voltage was converted to a varying frequency by a low power monolithic voltage-to-frequency converter operating at a center frequency of 4.1 k Hz. A signal of 0.25 μV at the electrodes caused a frequency change of 4 k Hz at the output of the VFC.

This figure assumes *maximum* gain, which occurred at a signal frequency of 3/4 Hz.

The overall noise performance of the electrodes and amplifier is shown in Figure 10. This shows the spectral level during the RISE experiment both before the transmitter was turned on and after it was off again. The noise includes, of course, geophysical noise sources in the water as well as amplifier and thermal agitation noises. The rise of noise level at low frequencies may be caused by voltages induced in the water by turbulent motions near the electrodes. The integrated noise in the frequency band of 0.25 - 0.75 Hz is about 2 nv r.m.s. Small eddies of diameter $d = 2$ cm and with water speeds u of a few millimeters/sec have induced voltages about udB at a frequency which depends on the speed with which they are convected past the electrodes; B is the geomagnetic induction, about 4×10^{-5}T. With the values chosen the voltage would be about one nanovolt and the frequency 1/2 Hz if the convection velocity is 1 cm/sec. It would be difficult to imagine that there is less activity near the electrodes. If this was indeed the source of noise we expected that it would be reduced, where the seafloor is sedimented, by driving the electrodes into the sediment, or by using electrodes of sufficient length that they integrate over a large number of eddies. On the other hand, electrodes as long as 0.9 m have been used subsequently by Webb and Cox (1984); their noise level is not markedly improved.

The signal strengths of the horizontal electric field components measured in the RISE experiment varied from 1 to 3×10^{-10} V/m at various transmitter frequencies between 0.25 and 2.25 Hz (Young, 1981). After integrating the signals by stacking for 504 seconds, the rms noise within individual frequency bands (see fig. 10) was 0.05 to 0.08×10^{-10} V/m. Thus a signal to noise ratio of 22 dB or more was achieved within a single stack and at a range of 18.9 km between source and receiver.

8. New Developments

An uncertainty has been introduced into the reported measurements by the discovery that, among a batch of unused electrodes, the electrode to electrode resistance (immersed in sea water) had increased from the initial value of 4 ohms to about 15 ohms. We attribute this increase to partial drying out of the electrodes which may have occurred before the experiment, or to the dissolution of the AgCl coating on the silver mesh. The gain of the amplifier at the low frequency end of the passband depends critically on the electrode resistance. Although it is probably possible to avoid the partial drying of electrodes, we believe some instability of electrode resistance is inevitable. Hence in recent work we have used amplifiers whose high input resistance is independent of frequency.

The system as described is limited in its ability to detect high resistance layers below the sea bed. This follows from the fact that signal frequencies comparable to one hertz are necessary to penetrate through the highly conductive, water-saturated basalt layer at the sea bed. If the materials underlying the basalt are much less conducting, then one must allow these signals to propagate a considerable horizontal distance before the attenuation and phase shifts associated with the underlying materials become appreciable. Therefore detection of high resistance materials demands greater ranges. Higher sensitivity receivers have been made with longer antennas. An antenna up to a kilometer in length is useful (if the skin depth in the high resistivity transmission path below the ocean is this large). However, the expense of deployment is large and the inherent geophysical noise limits the ultimate sensitivity (see Cox *et al.*, 1978; Webb and Cox, 1984). It is possible also to reduce the resistance of the receiver input section, thereby enhancing the signal relative to noise. By increasing the transmitted energy to 10 kw radiated for 5 days, and the receiver antenna length to 20 meters, the sensitivity could be improved to a level between curves b and c on Figure 2. This should permit detection of lithospheric materials as resistive as $10^5 ohm-m$ by reception of signals to a range of 70 km or more.

Acknowledgments

The funding for the development of this electromagnetic system was supplied by the Office of Naval Research/Earth Physics Program and the National Science Foundation/IDOE. We are indebted to Adam Schulz for preparation of the recorded data in plotted form and analysis of the noise and signal. The study of electrodes was supported by the Sea Grant program of the National Ocean and Atmospheric Agency.

REFERENCES

Baños, A., and J. R. Wesley (1953), The horizontal electric dipole in a conducting half space. Chapt. 4 of *Rept. no. 53-33*, Scripps Institution of Oceanography, M.P.L., Univ. California.

Cox, C. S. (1980), Electromagnetic induction in the oceans and inferences on the constitution of the earth, *Geophys. Surveys, 4*, 137-156.

Cox, C. S. (1981), On the electrical conductivity of the oceanic lithosphere, *Phys. Earth and Planetary Interiors, 25*, 196-102.

Cox, C. S., N. Kroll, P. Pistek, and K. Watson (1978), Electromagnetic fluctuations induced by wind waves on the deep sea floor, *J. Geophys. Res., 83*, 431-442.

Cox, C. S. *et al.* (7 authors) (1980), Atlantic lithospheric sounding, *J. Geomag. Geoelectr., 32*, Suppl. I, SI13-SI32.

Frieman, E. A., and N. M. Kroll (1973), Lithospheric propagation for undersea communication, *Tech. Rpt. (JASON) JSR-73-5*, Stanford Research Institute, Menlo Park, CA.

Ives, D. S. G., and G. J. Janz, editors (1961), *Reference Electrodes, Theory and Practice*, 651 pp., Academic Press, New York.

King, R.W.P., J.T. de Bettencourt, and B.H. Sandler (1979), Lateral wave propagation of electromagnetic waves in the lithosphere, *IEEE Trans. Geosci. Electr., GE-17*, 86-92.

Kraichman, M. B. (1970), *Handbook of Electromagnetic Phenomena in Conducting Media*, pp. 3-16, U.S. Government Printing Office, Washington, D.C.

Pistek, P. (1977), *Conductivity of the Ocean Crust*, Ph.D. Thesis, University of California San Diego, Scripps Institution of Oceanography.

Spiess, F. N. *et al.* (22 authors), 1980, East Pacific Rise: Hot springs and geophysical experiments, Science, 207, 1421-1433.

Wait, J. R. (1961), The electromagnetic fields of a horizontal dipole in the presence of a conducting half-space, *Can. Jour. Phys., 39*, 1017-1028.

Webb, S. and C. Cox (1982), Electromagnetic fields induced at the seafloor by Rayleigh-Stoneley waves, *J. Geophys. Res., 87*, 4093-4102.

Webb, S. and C. S. Cox (1984), Pressure and electric fluctuations on the deep seafloor: background noise for seismic detection, *Geophys. Res. Lett.* (submitted).

Young, P. D., 1981, *Anactive Source Electromagnetic Method for Probing the Earth's Electrical Conductivity Structure Below the Ocean Floor*, Ph.D. Thesis, University of California, San Diego, Scripps Institution of Oceanography. 231 pp.

Young, P. D. and C. S. Cox (1981), Electromagnetic active source sounding near the East Pacific Rise, *Geophys. Res. Lett., 8*(10), 1043-1046.

Figure 1

High frequency natural electric fields at the sea bed in deep water. One horizontal component of the field as measured on six meter antennas and sampled at 64 s intervals is shown at three stations represented by the traces 1A, 1B, 5. The stations were separated horizontally as shown in the inset. Observations were part of the "MODE" experiment in the Atlantic (Cox *et al.*, 1980). Note lack of coherence of highest frequency fields indicating short horizontal scale of these fields.

Figure 2

The horizontal EM field components on the sea bed as a function of horizontal range from an horizontal electric dipole antenna installed on the seafloor. The EM fields are computed along the axis of the dipole. The conductivity of the lithosphere is assumed to be uniform as shown in the inset in the middle panel.

Upper panel: The function $F(\gamma r)$ from eqs (1 and 2) for the field components E_r and B_ϕ.

Middle panel: the radial electric field at long ranges. Solid lines show signal strength for four source frequencies. Dashed lines show noise levels as follows:

a) Noise as in RISE experiment; integration time T = 504 sec. Source dipole strength p = 3 x 10^4 A m.

b) Similar to (a) except that T = 1 week, receiver antenna 20 m, p = 6 x 10^4 A m.

c) Noise reported by Cox *et al.* (1978) for 1 km antenna, T = 1 week, and p = 6 x 10^4 A m.

Lower panel: Tangential magnetic field B_ϕ per unit of source strength p. Solid lines show signal strength; dashed lines show noise levels estimated for flux gate magnetometer (d); induction type magnetic variometer (e); and superconducting magnetometer (f). Integration times and source dipole strength for noise levels (d-f) are T = 1 week and p = 6 x 10^4 A m.

Figure 3

HED source and receiver configuration for the RISE experiment. C is the coaxial cable; T is the transformer-rectifier transmitter; A is the antenna with bared electrodes at E; R is a receiver; crustal layers are numbered; MC is an hypothetical magma chamber. Insert shows a plan view of the site relative to the spreading center of the East Pacific Rise outlined by the central magnetic anomaly CMA and the 3000 m isobath.

Figure 4

Antenna current pulse shape. The rectangular form is the envelope of half sine wave loops of the rectified but unfiltered 60 Hz AC supply. The repetition period T could be varied from 1 to 4 seconds. The lower graph shows the amplitudes of harmonics 0-31 of the periodic envelope.

Figure 5

Receiver configuration. The spherical pressure case S contains all electronics and a tape recorder. The vacuum release chamber V holds S to the ballast weight B and the antennas A. Silver-silver chloride electrodes are at E. The separation between pairs of electrodes is 9 m. The instrument rests on tripod legs T. After release of ballast, S floats to the surface where beacon radios are activated. Their antennas are shown as BR.

Figure 6

Upper panel: Recorded voltages from unstacked, 4 second record.

Lower panel: Average recorded voltages from signals stacked over 126 sections of 4 second records. The data are identified by tape recorder frame numbers. During the recording of frames 126 and 127 the transmitter was operating with a repetition period of 4 seconds. The third harmonic is clearly evident in frame 126. During frame 54 the transmitter was off. Solid and dashed lines show the horizontal electric field components along azimuths of 48.5° and 318.5° respec-

tively, measured clockwise from magnetic north. The vertical bars indicate voltage scales at midband of the amplifiers (.75 Hz). Since the antenna lengths were both 9 m, the corresponding field intensity scales are 11 nV/m (upper panel) and 0.22 nV/m (lower panel).

Figure 7

Construction of the electrodes. The silver mesh Ag is supported by plastic rod P before being coated electrolytically with AgCl. It is surrounded by a mixture of diatomaceous earth and AgCl powder M within the porous thimble T and again isolated from water currents by diatomaceous earth D within crucible S. The junction J between silver and the insulated copper wire is covered in epoxy filling the cap C. The overall length of the electrode as shown is 200 mm.

Figure 8

The cross-hatched area shows the range of resistivity after electrolysis (electrodes: 5 cm x 14 cm silver mesh). Solid curve: Ag-electrodes without electrolytic process. The resistivity diminishes at high frequency because of reduced polarization. Measurements were made with current of 1 mA.

Figure 9

Schematic diagram of amplifier.

Figure 10

Noise level as recorded at the sea bed. The right hand scale shows the inferred electric field noise for a 9 m antenna. The vertical bar shows the 95% confidence interval of the spectrum.

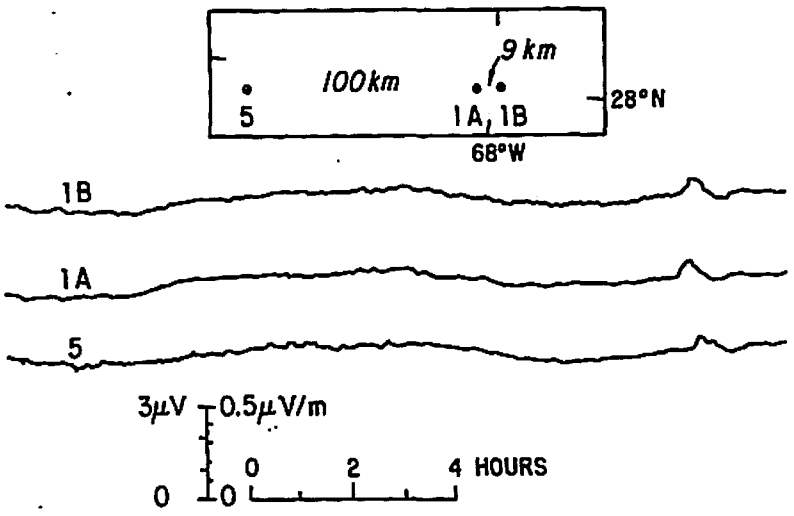

Figure 1

High frequency natural electric fields at the sea bed in deep water. One horizontal component of the field as measured on six meter antennas and sampled at 64 s intervals is shown at three stations represented by the traces 1A, 1B, 5. The stations were separated horizontally as shown in the inset. Observations were part of the "MODE" experiment in the Atlantic (Cox *et al.*, 1980). Note lack of coherence of highest frequency fields indicating short horizontal scale of these fields.

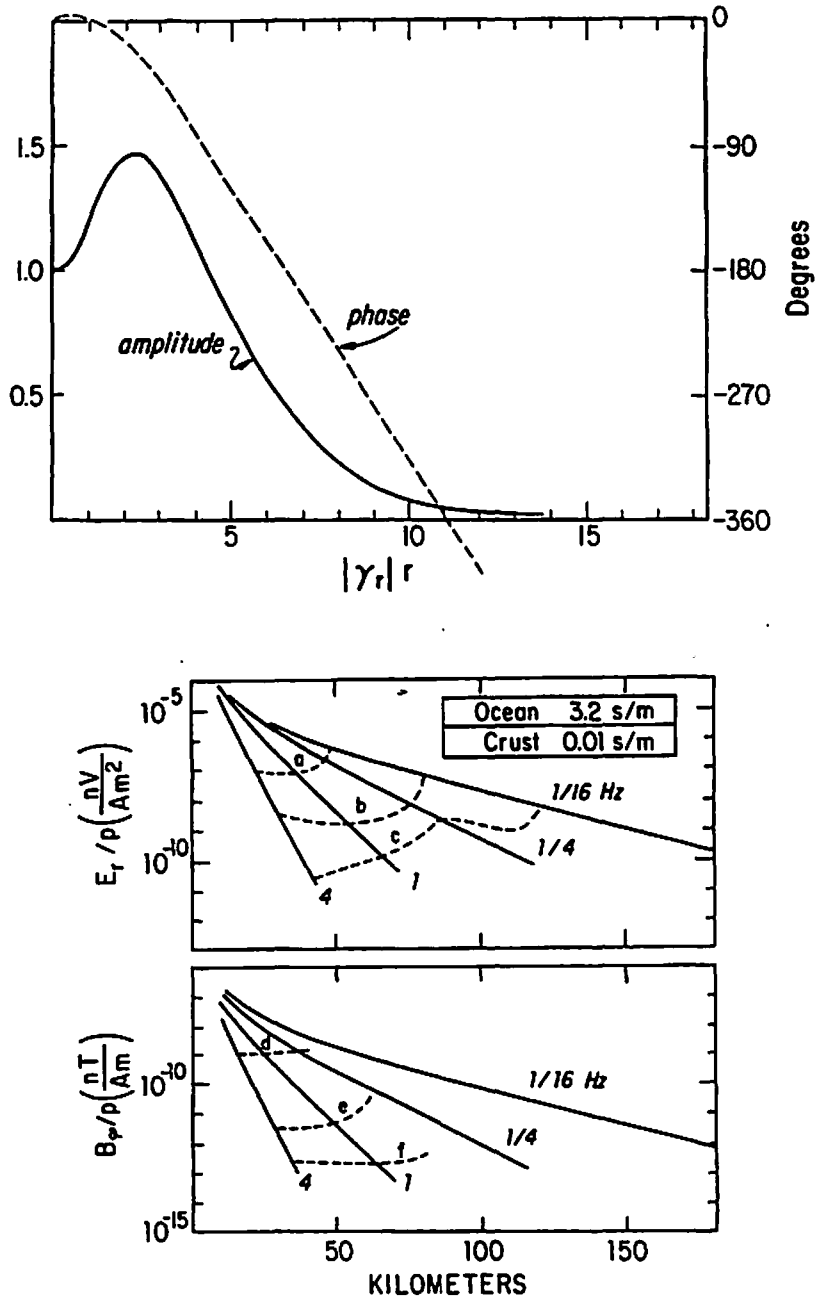

Figure 2

The horizontal EM field components on the sea bed as a function of horizontal range from an horizontal electric dipole antenna installed on the seafloor. The EM fields are computed along the axis of the dipole. The conductivity of the lithosphere is assumed to be uniform as shown in the inset in the middle panel.

Upper panel: The function $F(\gamma r)$ from eqs (1 and 2) for the field components E_r and B_ϕ.

Middle panel: the radial electric field at long ranges. Solid lines show signal strength for four source frequencies. Dashed lines show noise levels as follows:

a) Noise as in RISE experiment; integration time T = 504 sec. Source dipole strength p = 3 x 10^4 A m.

b) Similar to (a) except that T = 1 week, receiver antenna 20 m, p = 6 x 10^4 A m.

c) Noise reported by Cox *et al.* (1976) for 1 km antenna, T = 1 week, and p = 6 x 10^4 A m.

Lower panel: Tangential magnetic field B_ϕ per unit of source strength p. Solid lines show signal strength; dashed lines show noise levels estimated for flux gate magnetometer (d); induction type magnetic variometer (e); and superconducting magnetometer (f). Integration times and source dipole strength for noise levels (d-f) are T = 1 week and p = 6 x 10^4 A m.

TABLE I

Geometrical effects on resistance of electrodes. The resistance between the electrode and infinity is compared for 3 shapes of electrodes immersed in a uniform fluid of resistivity ρ.

Shape	Resistance R	Area and volume of electrode	Figures of Merit $\rho/(R A^{1/2})$	Figures of Merit $\rho/(R V^{1/3})$
Sphere of radius a	$\rho/(4\pi a)$	$A = 4\pi a^2 \qquad V = (4/3)\ a^3$	$2\pi^{1/2} = 3.54$	$3^{1/3}(4\pi)^{2/3} = 7.80$
Disk of radius a	$\rho/(8\ a)$	$A = \pi a^2$	$8/\pi^{1/2} = 4.51$	
Prolate spheroid (semimajor axis c, semiminor axis a)	$[\rho/(8\pi\sqrt{c^2-a^2})]\ln\left[\frac{c+\sqrt{c^2-a^2}}{c-\sqrt{c^2-a^2}}\right]$	$A = 2\pi a^2\left[1 + \frac{\sin^{-1}\sqrt{1-a^2/c^2}}{(a/c)\sqrt{1-a^2/c^2}}\right] \qquad V=\frac{4\pi}{3}a^2c$		
Prolate spheroid $a/c \ll 1$	$[\rho/(4\pi c)]\ln(2c/a)$	$A = \pi^2 a\ c \qquad V = \frac{4}{3}\pi a^2 c$	$\frac{4(c/a)^{1/2}}{\ln(2c/a)}$	$\frac{3^{1/3}(4\pi^{2/3}c/a)^{2/3}}{\ln(2c/a)} = \frac{7.8(c/a)^{2/3}}{\ln(2c/a)}$
Transmitter electrode $a/c = 8.7 \times 10^{-4}$			17.5	111.
Receiver electrode $a/c = 7.3 \times 10^{-2}$			4.5	13.5

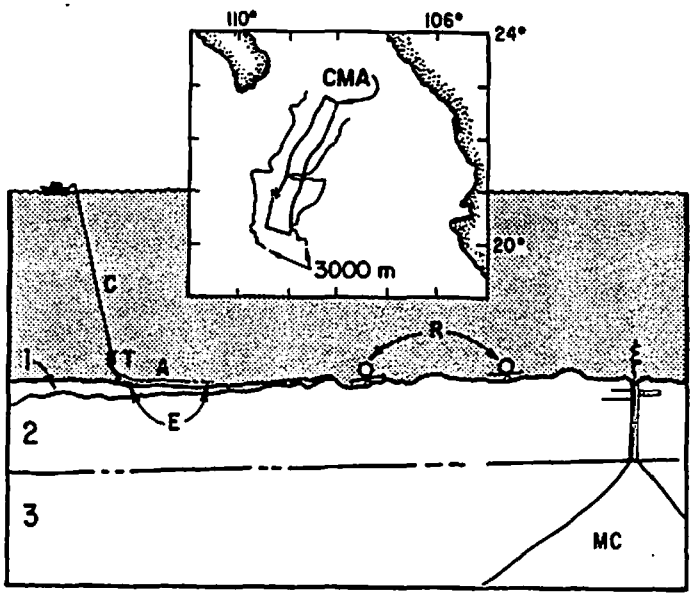

Figure 3

HED source and receiver configuration for the RISE experiment. C is the coaxial cable; T is the transformer-rectifier transmitter; A is the antenna with bared electrodes at E; R is a receiver; crustal layers are numbered; MC is an hypothetical magma chamber. Insert shows a plan view of the site relative to the spreading center of the East Pacific Rise outlined by the central magnetic anomaly CMA and the 3000 m isobath.

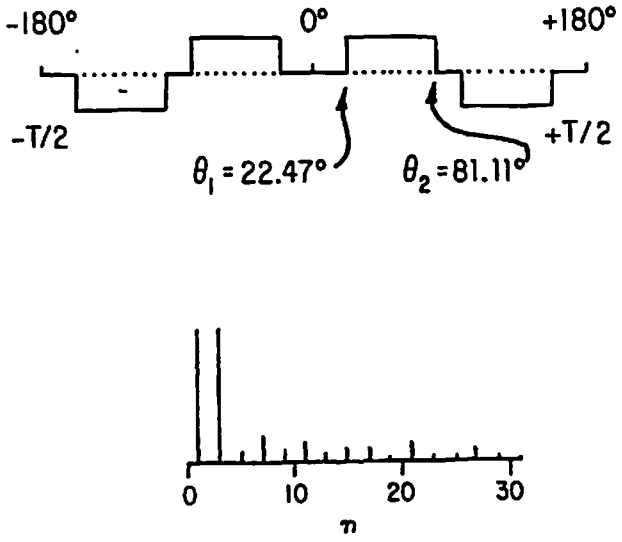

Figure 4

Antenna current pulse shape. The rectangular form is the envelope of half sine wave loops of the rectified but unfiltered 60 Hz AC supply. The repetition period T could be varied from 1 to 4 seconds. The lower graph shows the amplitudes of harmonics 0-31 of the periodic envelope.

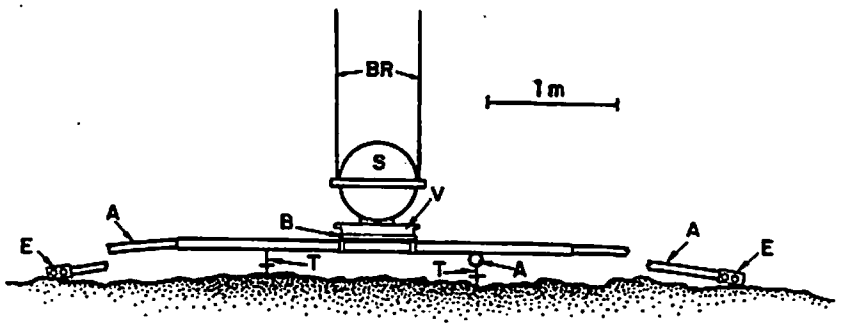

Figure 5

Receiver configuration. The spherical pressure case S contains all electronics and a tape recorder. The vacuum release chamber V holds S to the ballast weight B and the antennas A. Silver-silver chloride electrodes are at E. The separation between pairs of electrodes is 9 m. The instrument rests on tripod legs T. After release of ballast, S floats to the surface where beacon radios are activated. Their antennas are shown as BR.

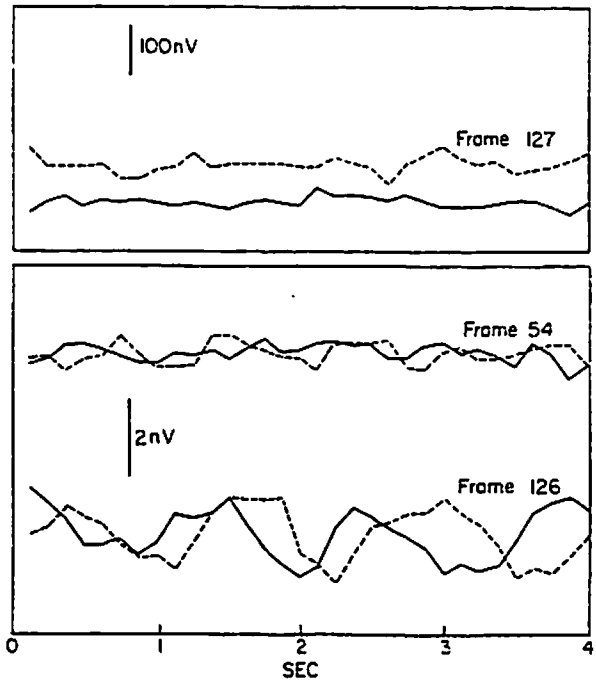

Figure 6

Upper panel: Recorded voltages from unstacked, 4 second record.

Lower panel: Average recorded voltages from signals stacked over 126 sections of 4 second records. The data are identified by tape recorder frame numbers. During the recording of frames 126 and 127 the transmitter was operating with a repetition period of 4 seconds. The third harmonic is clearly evident in frame 126. During frame 54 the transmitter was off. Solid and dashed lines show the horizontal electric field components along azimuths of 46.5° and 316.5° respectively, measured clockwise from magnetic north. The vertical bars indicate voltage scales at midband of the amplifiers (.75 Hz). Since the antenna lengths were both 9 m, the corresponding field intensity scales are 11 nV/m (upper panel) and 0.22 nV/m (lower panel).

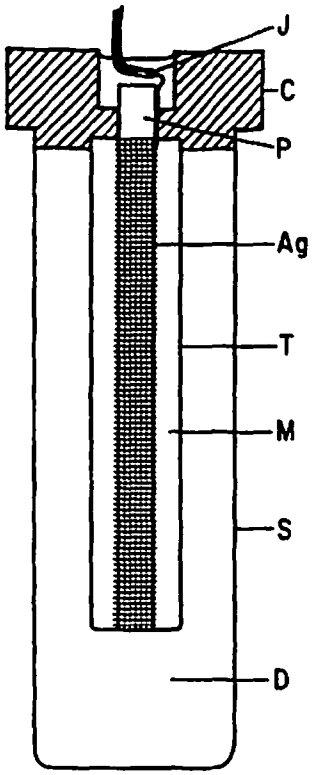

Figure 7

Construction of the electrodes. The silver mesh Ag is supported by plastic rod P before being coated electrolytically with AgCl. It is surrounded by a mixture of diatomaceous earth and AgCl powder M within the porous thimble T and again isolated from water currents by diatomaceous earth D within crucible S. The junction J between silver and the insulated copper wire is covered in epoxy filling the cap C. The overall length of the electrode as shown is 200 mm.

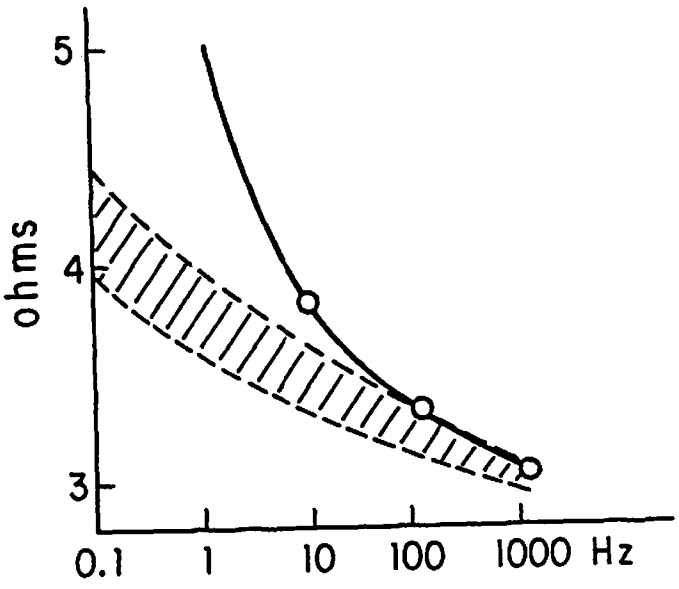

Figure 8

The cross-hatched area shows the range of resistivity after electrolysis (electrodes: 5 cm x 14 cm silver mesh). Solid curve: Ag-electrodes without electrolytic process. The resistivity diminishes at high frequency because of reduced polarization. Measurements were made with current of 1 mA.

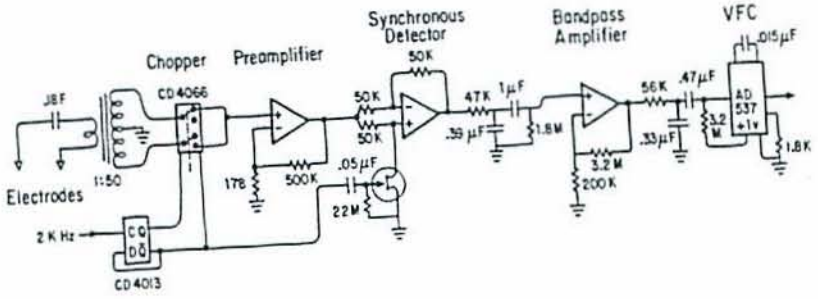

Figure 9

Schematic diagram of amplifier.

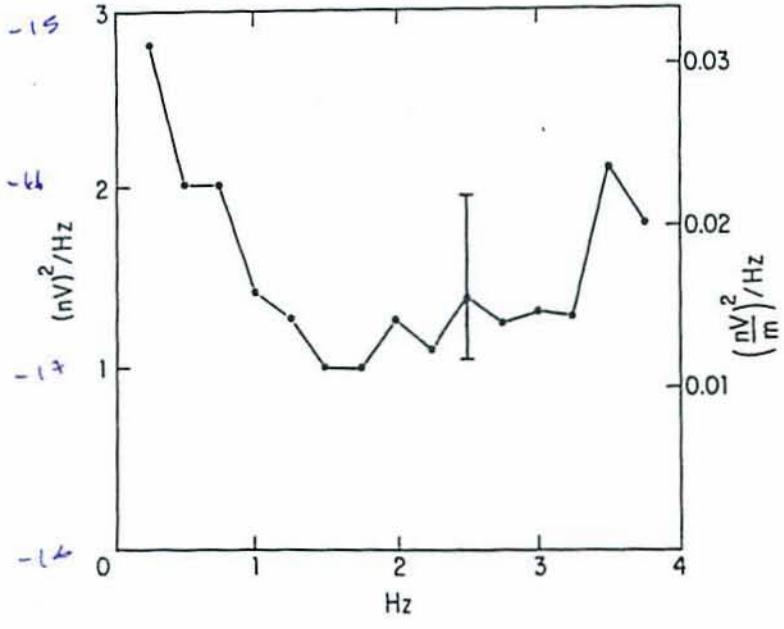

Figure 10

Noise level as recorded at the sea bed. The right hand scale shows the inferred electric field noise for a 9 m antenna. The vertical bar shows the 95% confidence interval of the spectrum.